



Since January 2020 Elsevier has created a COVID-19 resource centre with free information in English and Mandarin on the novel coronavirus COVID-19. The COVID-19 resource centre is hosted on Elsevier Connect, the company's public news and information website.

Elsevier hereby grants permission to make all its COVID-19-related research that is available on the COVID-19 resource centre - including this research content - immediately available in PubMed Central and other publicly funded repositories, such as the WHO COVID database with rights for unrestricted research re-use and analyses in any form or by any means with acknowledgement of the original source. These permissions are granted for free by Elsevier for as long as the COVID-19 resource centre remains active.



Novel mannopyranoside esters as sterol 14 α -demethylase inhibitors: Synthesis, PASS predication, molecular docking, and pharmacokinetic studies

Mohammed M. Matin^{a,*}, Priyanka Chakraborty^a, Muhammad S. Alam^b, Mohammad M. Islam^c, Umme Haneef^a

^a Biorganic and Medicinal Chemistry Laboratory, Department of Chemistry, Faculty of Science, University of Chittagong, Chattogram, 4331, Bangladesh

^b Molecular Modeling & Drug Design Laboratory, Bangladesh Council of Scientific & Industrial Research (BCSIR) Laboratories, Chattogram, 4220, Bangladesh

^c Department of Biochemistry and Molecular Biology, Faculty of Biological Science, University of Chittagong, Chattogram, 4331, Bangladesh

ARTICLE INFO

All front fighters and researchers against COVID-19 to save the mankind

Keywords:

Methyl α -D-mannopyranoside esters
Acylation
Antifungal agents
Sterol 14 α -demethylase (CYP51) inhibitor
Molecular docking
Pharmacokinetic studies

ABSTRACT

Direct unimolar one-step valeroylation of methyl α -D-mannopyranoside (MDM) furnished mainly 6-O-valeroate. However, similar reaction catalyzed by DMAP resulted 3,6-di-O-valeroate (21%) and 6-O-valeroate (47%) indicating reactivity sequence as 6-OH > 3-OH > 2-OH, 4-OH. To get potential antimicrobial agents, 6-O-valeroate was converted into four 2,3,4-di-O-acyl esters, and 3,6-di-O-valeroate was converted into 2,4-di-O-acetate. Direct tetra-O-valeroylation of MDM gave a mixture of 2,3,4,6-tetra-O-valeroate and 2,3,6-tri-O-valeroate indicating that the C2-OH is more reactive than the equatorial C4-OH. The activity spectra analysis along with *in vitro* antimicrobial evaluation clearly indicated that these novel MDM esters had better antifungal activities over antibacterial agents. In this connection, molecular docking indicated that these MDM esters acted as competitive inhibitors of sterol 14 α -demethylase (CYP51), an essential enzyme for clinical target to cure several infectious diseases. Furthermore, pharmacokinetic studies revealed that these MDM esters may be worth considering as potent candidates for oral and topical administration. Structure activity relationship (SAR) affirmed that saturated valeric chain (C5) in combination with caprylic (C8) chains was more promising CYP51 inhibitor over conventional antifungal antibiotics.

1. Introduction

Fatty acid esters of monohydric alcohols such as methanol or ethanol have been reported to be associated with reduced antimicrobial activity of fatty acids [1]. On the other hand, fatty acid esters of the polyhydric glycerol, i.e. monolaurin, have been found to increase their effectiveness as antimicrobial agent [2]. Accordingly, fatty acid esters of sugars with multiple hydroxyl groups constituted an important class of fatty acid derivatives, termed carbohydrate fatty acid (CFA) esters and/or sugar esters (SEs) [3]. These tasteless, and odorless SEs are composed of a hydrophilic carbohydrate moiety, and one or more fatty acids as lipophilic moieties [4]. Therefore, SEs are amphiphilic, nontoxic, biodegradable, nonirritating, and environment friendly [5]. In addition, the good stabilizing, and conditioning properties of CFA esters significantly contributed to their increased inclusion in daily commodities including as low caloric sweeteners, fat replacer, flavorings, and

biosurfactants/emulsifiers in foods, food additives, detergents, and in pharmaceutical, biomedical, cosmetic, and oral-care products [6,7].

The properties of CFA esters can vary widely from a minute changes in their constituent fatty acid, and sugar moieties and therefore, it is of immense interest to develop CFA esters of diverse physicochemical properties with various biological functions. For examples, several CFA esters have reported to have antitumor, plant growth inhibitory, insecticidal, and mitocidal, antibiotic, and antifriction property [8–12]. Therefore, CFA esters have long been used as versatile intermediates in the syntheses of many natural products due to the presence of multifunctional groups [13–15], in addition to their extensive use for design, and development of new drugs [16].

In recent decades, emergence of multiple drug resistant (MDR) pathogenic strains is a global health concern, a leading cause of nosocomial, and community infections [17]. Therefore, design and synthesis of new chemotherapeutic agents with novel mode of action is always

* Corresponding author.

E-mail address: mahbubchem@cu.ac.bd (M.M. Matin).

<https://doi.org/10.1016/j.carres.2020.108130>

Received 3 July 2020; Received in revised form 2 August 2020; Accepted 9 August 2020

Available online 14 August 2020

0008-6215/© 2020 Elsevier Ltd. All rights reserved.

time-demanding dealing with MDR microbial strains. The structure activity relationship (SAR) of several mannopyranose esters with different side chains concluded that 6-*O*-myristoyl- α -mannopyranose [(Fig. 1(1))] was highly active against methicillin-resistant *Staphylococcus aureus* ATCC 33591 (MRSA), in addition to its prospective use as environment friendly antimicrobial in food processing, food preservation, and for treating bacterial and fungal diseases in animal, and plants [18]. Very recently, we reported that incorporation of alkanoyl, and aromatic ester groups on octyl glucopyranoside [Fig. 1(2)] as carbohydrate moiety increased antimicrobial potentiality even at very low concentration ($10 \mu\text{g mL}^{-1}$) which may act as competitive inhibitors of lanosterol 14 α -demethylase [19].

Synthesis of CFA esters can be achieved by chemical and enzymatic methods, and industrial sugar esters are currently being manufactured by chemical syntheses. However, the two major challenges with CFA ester syntheses are- (i) the presence of several 2° hydroxyl groups of almost similar reactivity, mostly affecting functionalization (esterification) step leading to a mono-, di-, and polyesters [20], and (ii) the tremendous variation (variety) of carbohydrate structures. Accordingly, various methods have been attempted and reported in the last couple of decades for selective esterification (acylation) [21–32]. All the methods and/or strategies described were successful to some extents, however, suffered from numerous shortcomings, i.e. complex processes of multiple steps, tedious, expensive, low selectivity and extremely low yield [32,33]. Hence, in most of the cases, direct acylation method maintaining proper reaction conditions is preferred for the monosaccharide-based CFA ester synthesis to reduce the number of steps, and to increase the final yield(s) [23,29].

Most of the antifungal and antiprotozoal drugs are designed through targeting sterol 14 α -demethylase (CYP51) inhibition [34] such as azoles (fluconazole; VNI; Fig. 2). Inactivity of CYP51 deters the biosynthesis of fungal essential ergosterol [34b]. However, MDR to azole class needs to identify non-azole scaffolds with high affinity for CYP51 [35]. Antimicrobial activities especially antifungal susceptibility of CFA esters is also related to CYP51 inhibition [19,22] similar to azoles, papulacandins etc. In addition, sugar moieties with ester groups as in papulacandins led to higher solubility and reduced hemolytic toxicity [36]. Hence, one of our major objectives was to get non-azole type MDM based potential CYP51 inhibitor to overcome MDR microbial strains.

Even though the broad applications of SEs are known for many years, huge variation of their antimicrobial activities is one of the major drawbacks, and in addition, detail pharmacokinetic studies along with SAR were missing. In this study, we aimed at regioselective synthesis of valeroyl esters of MDM [Fig. 1(3)] employing direct and DMAP-catalyzed method, and successfully synthesized nine MDM esters [Fig. 2(4–12)]. The detail investigation of PASS (prediction of activity spectra for substances), *in vitro* antimicrobial activities, molecular docking with sterol 14 α -demethylase (CYP51), MM-GBSA binding affinity analyses, and pharmacokinetic calculations (ADME/T, drug-likeness) including SAR for competitive CYP51 inhibitors of 4–12 are discussed.

2. Results and discussion

2.1. Regioselective 6-*O*-valeroylation of mannopyranoside

Initially, methyl α -D-mannopyranoside (MDM, 3) was reacted with valeroyl chloride in dry pyridine at low temperature for 18 h, followed

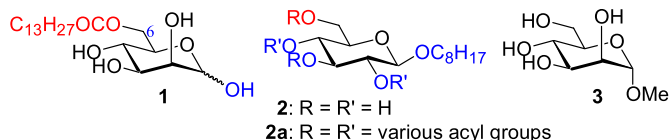


Fig. 1. Structure of compounds 1–3.

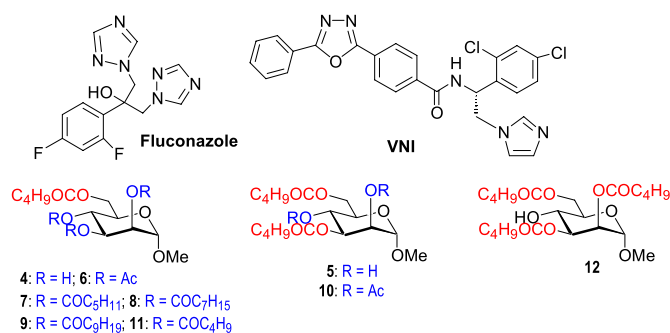
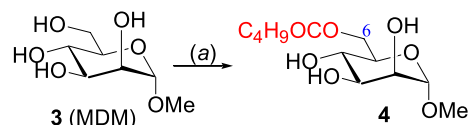


Fig. 2. Synthesized MDM SEs, fluconazole, and VNI.



Scheme 1. Reagents and conditions: (a) Py, $\text{C}_4\text{H}_9\text{COCl}$, 0°C -r-t, 18 h, 79%.

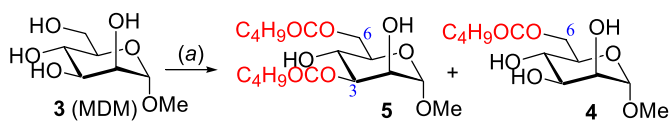
by chromatographic purification gave a semi-solid (Scheme 1).

Stretching bands at 3250–3550 (br, OH), 1733 (CO), 1059 cm^{-1} (pyranose ring) in its FT-IR spectrum indicated the attachment of only one valeroyl group with MDM molecule (Fig. S1). The ^1H NMR spectrum clearly showed a two-proton triplet at δ 2.37 ($J = 7.4 \text{ Hz}$), two two-proton multiplets at δ 1.55–1.64 and 1.30–1.40, and a three-proton triplet at δ 0.91 ($J = 7.4 \text{ Hz}$) indicating the attachment of one valeroyloxy group in the molecule. In addition, H-6a (at δ 4.40 as dd, $J = 12.2$ 5.0 Hz) and H-6b (at δ 4.22–4.32 as br m) resonated considerable downfield as compared to its precursor MDM (usual value for H-6a is $\delta \sim 3.85$ and for H-6b is $\delta \sim 3.75$) [37,38] which clearly demonstrated the incorporation of valeroyloxy group at C-6 position. This observation was furthermore confirmed by the HMBC spectrum (Fig. S8). The ^{13}C NMR spectrum showed the presence of only one carbonyl peak at δ 174.1, and four additional aliphatic carbon signals at δ 34.1, 26.9, 22.2 and 13.6. Altogether the FT-IR, ^1H & ^{13}C NMR, COSY, and HMBC spectra (Figs. S1–S10) unambiguously confirmed the MDM ester as methyl 6-*O*-valeroyl- α -D-mannopyranoside (4).

2.2. DMAP-catalyzed valeroylation: synthesis of methyl 3,6-di-*O*-valeroyl- α -D-mannopyranoside (5) and methyl 6-*O*-valeroyl- α -D-mannopyranoside (4)

Unimolar valeroylation of MDM (3) in presence of 4-dimethylaminopyridine (DMAP) in pyridine at low temperature gave two faster moving products with $R_f = 0.59$ and $R_f = 0.31$ (chloroform/methanol = 5:1; Scheme 2). Initial elution with chloroform/methanol provided the faster-moving component ($R_f = 0.59$) in 21% as a semi-solid which resisted crystallization.

This semi-solid component showed bands at 3300–3600 (br), 1747, 1718 and 1062 cm^{-1} in FT-IR spectrum, corresponding to OH, CO and pyranose ring stretching, respectively. These observations indicated the partial attachment of valeroyl groups in MDM molecule. Further, the ^1H NMR showed extra eighteen aliphatic characteristic protons corresponded to two valeroyl groups, and thus, confirmed the attachment of two valeroyloxy groups in the molecule, which was furthermore, corroborated by ^{13}C NMR spectra; two carbonyl peaks appeared at δ 174.1 and 173.5. The reasonable downfield shift of H-3 to δ 5.11 (as dd) from its usual value $\sim \delta$ 3.89 ppm [37], and H-6 to δ 4.54 (1H as dd), and 4.31 (1H as dd) as compared to 3 [38,39] clearly suggested the attachment of valeroyl groups at C-3 and C-6 positions. These altogether observations (Figs. S11–S15), assigned the synthesized MDM ester as methyl 3,6-di-*O*-valeroyl- α -D-mannopyranoside (5).



Scheme 2. Reagents and conditions: (a) Py, C_4H_9COCl , DMAP, 0 °C-rt, 16 h, 5 (21%), 4 (47%).

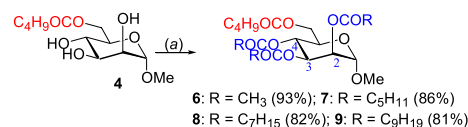
Furthermore, elution with chloroform/methanol (15:1) provided the slower-moving component ($R_f = 0.31$) in 47% yield as a semi-solid (Scheme 2). This compound was found completely identical as prepared earlier by direct method, and hence, assigned as 6-*O*-valeroate 4. Formation of 3,6-di-*O*-valeroate 5, and 6-*O*-valeroate 4 demonstrated that during DMAP-catalyzed valeroylation reactivity of OH groups in MDM is: 6-OH > 3-OH > 2-OH, 4-OH.

Let us consider the mechanism for 3,6-di-*O*-valeroate 5 formation under DMAP-catalyzed reaction; *N*-acyl(4-dimethylamino)pyridinium ion selectively attacks the less hindered equatorial C3 OH position of the initially formed 6-*O*-valeroate 4, as evident by similar type of previous observation [40]. The abstraction of a proton from the complex 4a by pyridine facilitates removal of DMAP to produce compound 5 (Fig. 3).

2.3. Synthesis of 2,3,4-tri-*O*-acyl esters of 6-*O*-valeroate 4

To confirm the structure of 6-*O*-valeroate 4 and to get new CFA esters with various chain length (C2–C10) we have synthesized four 2,3,4-tri-*O*-acyl esters 6–9 employing acetic anhydride, hexanoyl chloride, octanoyl chloride and decanoyl chloride. Initially, 2,3,4-triol 4 on reaction with acetic anhydride in anhydrous pyridine in the presence of DMAP for 11 h afforded a faster moving single product compound as a thick syrup (93% yield; Scheme 3)

The FT-IR spectrum analysis of this syrup clearly showed four carbonyl stretching peaks at 1759, 1755, 1753, and 1738 cm^{-1} . Furthermore, the frequency corresponding to OH group(s) was absent, indicating the tri-*O*-acetylation of the molecule. The 1H NMR spectrum indicated a three-proton singlet at δ 3.42 (assigned for anomeric OCH_3 protons), and three three-proton singlets at δ 2.16, 2.05 and 2.00 (assigned as acetyl methyl protons). The H-2, H-3 and H-4 protons appeared at δ 5.25, 5.35 and 5.29, respectively while those were at δ 3.92, 3.78 and 3.64, respectively in its precursor 6-*O*-valeroate 4. These downfield shifts confirmed the attachment of acetoxy groups at C-2, C-3 and C-4 positions. These were further affirmed by its ^{13}C NMR spectra;



Scheme 3. Reagents and conditions: (a) Py, $Ac_2O/RCOCl$, DMAP, 0 °C-rt, 11–16 h.

three acetyl carbonyl peaks appeared at δ 170.0, 169.8, and 169.6, along with three acetyl methyl carbons resonated at δ 20.8, 20.7, and 20.6. Therefore, the structure of the acetate was assigned as methyl 2,3,4-tri-*O*-acetyl-6-*O*-valeroyl- α -D-mannopyranoside (6; Figs. S16–S20).

Further reaction of 4 with 3.3 molar equivalent hexanoyl chloride in pyridine in the presence of DMAP for 14 h followed by chromatography gave a semi-solid product (86% yield; Scheme 3). This semi-solid product had four bands at 1739, 1725, 1713, and 1695 cm^{-1} for CO group, and no bands were observed for OH group, indicating that the attachment of hexanoyl groups in the molecule. This interpretation was furthermore supported by the 1H and ^{13}C NMR spectra (Figs. S21–S25); 1H NMR showed the characteristic extra thirty-three protons (equivalent in numbers to three hexanoyl groups added to the molecule) in addition to valeroyl's nine protons. These observations unambiguously established the newly synthesized compound as methyl 2,3,4-tri-*O*-hexanoyl-6-*O*-valeroyl- α -D-mannopyranoside (7).

Similarly, separate reaction of triol 4 with 3.3 molar equivalent octanoyl chloride and decanoyl chloride followed by chromatography gave 2,3,4-tri-*O*-octanoate 8 (Fig. S26–S30), and 2,3,4-tri-*O*-decanoate 9 (Figs. S31–S35), respectively in good yields (Scheme 3).

2.4. Synthesis of methyl 2,4-di-*O*-acetyl-3,6-di-*O*-valeroyl- α -D-mannopyranoside 10

In compound 5, C-2 and C-4 OH groups are free. We have exploited these positions for acetylation employing dimolar acetic anhydride. Thus, treatment of 3,6-di-*O*-valeroate 5 with acetic anhydride in pyridine in the presence of catalytic amount of DMAP yielded a syrup in 89% yield (Scheme 4).

The FT-IR spectrum of the reaction product showed characteristic peaks at 1763, 1756, 1747, 1733 (CO), and 1086 cm^{-1} while the stretching band for OH group(s) was absent, indicating the complete acetylation of 3,6-di-*O*-valeroate 5. The 1H NMR spectrum of the

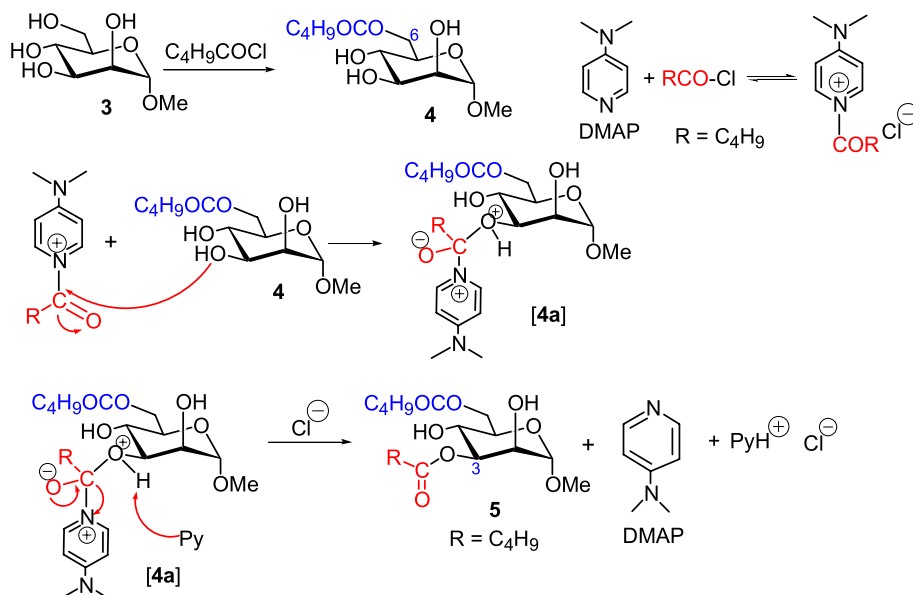


Fig. 3. Mechanism for the formation of DMAP-catalyzed 3,6-di-*O*-valeroate 5.

compound had two additional three-proton singlets at δ 2.15 and 2.03, and the ^{13}C NMR spectrum indicated two additional carbonyl (CO) signals at δ 169.9 and 169.6, and two methyl carbon signals at δ 20.7 and 20.6, together confirmed the attachment of two acetyl groups in this compound. Furthermore, a downfield shift of H-2 (δ 5.24) and H-4 (δ 5.31) indicated the attachment of acetyl group at C-2 and C-4 positions, respectively, fully corroborating with the HMBC experiments. Therefore, all these observations, together assigned the structure of compound as methyl 2,4-di-*O*-acetyl-3,6-di-*O*-valeroyl- α -D-mannopyranoside (**10**; Figs. S36–S44).

2.5. Synthesis of per-*O*-valeroyl esters of MDM (**3**)

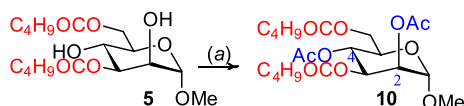
To compare biological activities and to examine positional effect of acyl groups we extended direct acylation method to prepare per-*O*-valeroyl MDM; treatment of **4** with little excess valeroyl chloride for 14 h followed by chromatographic purification gave a homogeneous syrup (91%; Scheme 5). On the basis of its ^1H NMR (which showed attachment of additional 27 protons) and other spectroscopic analyses (Figs. S45–S50) the compound was unambiguously established as methyl 2,3,4,6-tetra-*O*-valeroyl- α -D-mannopyranoside (**11**).

On the other hand, direct valeroylation of **3** with excess valeroyl chloride showed sluggish reaction and hence we increased temperature up to 45 °C. After 16 h work-up followed by purification yielded major faster-moving compound ($R_f = 0.58$, 56%) along with slower-moving compound ($R_f = 0.49$, 26%; Scheme 5). The FT-IR, ^1H and ^{13}C NMR spectra of higher R_f compound were found identical to that of the compound **11** prepared from 6-*O*-pentanoate **4**. The slower-moving minor compound showed characteristic OH bands at 3308–3560 cm^{-1} in its FT-IR spectrum. The presence of OH stretching band indicated the partial valeroylation of MDM molecule. Appearance of extra twenty-seven protons (three valeroxyloxy groups), and three CO peaks in its ^1H and ^{13}C NMR spectrum, respectively as well as considerable downfield shift of H-2, H-3, and H-6 as compared to **3** [38,39] confirmed the attachment of valeroyl group at C-2, C-3, and C-6 positions. Thus, it was assigned as methyl 2,3,6-tri-*O*-valeroyl- α -D-mannopyranoside (**12**; Figs. S51–S56).

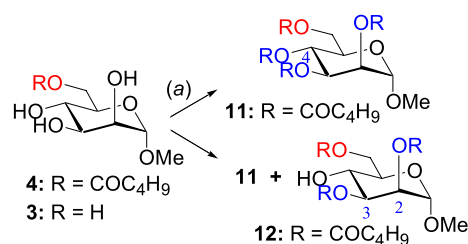
Formation of 2,3,6-tri-*O*-valeroate **12** from MDM (**3**) further proved that 4-OH is the least reactive among OH groups in MDM. Thus, along with our previous observation as described in earlier sections for regioselective valeroylation by direct, and DMAP-catalyzed method, we can conclude that the reactivity of all OH groups in MDM (**3**) follow the order: 6-OH > 3-OH > 2-OH > 4-OH.

2.6. Computational antimicrobial activities evaluation using PASS

Web based PASS (prediction of activity spectra for substances; <http://www.pharmaexpert.ru/PASSonline/index.php>) was used for the evaluation of antimicrobial activities of the compounds, as reported previously [27]. The PASS prediction data of the mannopyranoside derivatives **4–12** clearly indicated that the MDM esters reported here had reasonable antimicrobial activities (Table 1). However, the predicted biological activities against bacteria ($0.52 < \text{Pa} < 0.58$) and fungi ($0.62 < \text{Pa} < 0.71$) clearly suggested that the MDM esters could be more potent against phytopathogenic fungi as compared to that against bacterial pathogens. The PASS study also revealed that compounds identified from the present study have various potential biological activities, and further studies are needed to validate these predictions.



Scheme 4. Reagents and conditions: (a) Py, Ac_2O , DMAP, 0 °C-rt, 11 h, 89%.



Scheme 5. Reagents and conditions: (a) **4**, Py, $\text{C}_4\text{H}_9\text{COCl}$, DMAP, 0–45 °C, 14 h, 91%; (b) **3**, Py, $\text{C}_4\text{H}_9\text{COCl}$, DMAP, 0–45 °C, 16 h, **11**: 56% & **12**: 26%.

Table 1

PASS predicted biological activity of MDM esters.

Drug	Biological Activity			
	Antibacterial		Antifungal	
	Pa	Pi	Pa	Pi
3	0.541	0.013	0.627	0.016
4	0.528	0.014	0.669	0.012
5	0.570	0.011	0.706	0.009
6	0.558	0.012	0.675	0.011
7	0.551	0.012	0.673	0.011
8	0.551	0.012	0.673	0.011
9	0.551	0.012	0.673	0.011
10	0.574	0.010	0.692	0.010
11	0.551	0.012	0.673	0.011
12	0.578	0.010	0.699	0.010

Pa = Probability 'to be active'; Pi = Probability 'to be inactive'

2.7. In vitro antimicrobial activities of MDM esters **4–12**

2.7.1. Effects against bacteria

The antibacterial activities of the MDM esters were evaluated against one Gram-positive (*Staphylococcus aureus*), and two Gram-negative (*Escherichia coli* and *Pseudomonas aeruginosa*) bacteria using disc diffusion method (diameter in mm; Table 2; Fig. 4a). None of the compounds showed any observable antibacterial effects against Gram-negative bacterial while all compounds had very similar antibacterial effects against Gram-positive *Staphylococcus aureus* (Table 2). Effectiveness against Gram-positive *S. aureus* (MRSA) was previously observed for mannose monoester **1** in pyranose form [18]. However, the present MDM ester series (pyranoside form) showed little activity against MRSA probably due to more lipophilicity (presence of multiple acyl chains) and glycosidic nature.

Table 2

Antibacterial effects of MDM esters **4–12**.

Type→ Drug	Diameter of zone of inhibition in mm (5 μg .dw/disc)		
	G-(+ve) <i>S. aureus</i>	G(-ve) <i>E. coli</i>	G(-ve) <i>P. aeruginosa</i>
3	08 ± 0.50	NI	NI
4	08 ± 0.50	NI	NI
5	09 ± 1.00	NI	NI
6	09 ± 0.55	NI	NI
7	09 ± 0.35	NI	NI
8	09 ± 0.50	NI	NI
9	09 ± 0.35	NI	NI
10	08 ± 0.70	NI	NI
11	09 ± 0.45	NI	NI
12	08 ± 0.60	NI	NI
TC ^[a]	*22 ± 0.58	*25 ± 0.50	*22 ± 0.41

Data are presented as Mean ± SD. TC = tetracycline; NI = no inhibition; dw = dry weight; * = good inhibition; [a] standard antibiotic (25 μg /disc).

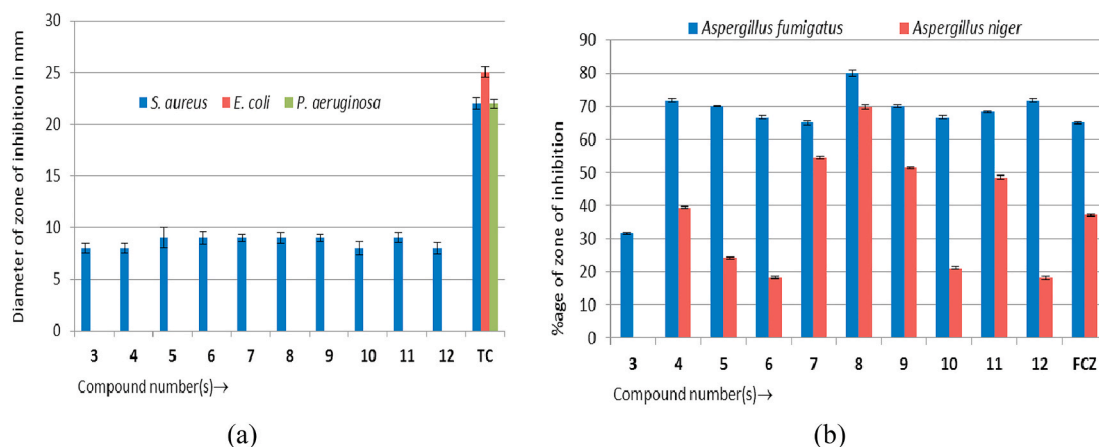


Fig. 4. (a) Diameter of zone of inhibition in mm against bacteria (TC = tetracycline), (b) %age of inhibition against fungal pathogens (FCZ = fluconazole).

2.7.2. Antifungal activities

The evaluation of *in vitro* antifungal activities [9] of MDM esters 4–12 against two pathogenic fungi viz. *Aspergillus fumigatus* ATCC 46645, and *Aspergillus niger* ATCC 16404 clearly indicated that all the MDM esters had excellent antifungal activities (Table 3; Fig. 4b). To be more precise, the antifungal activities of MDM esters were very similar and/or even better than that observed with standard antibiotic fluconazole (Table 3) against *A. fumigatus*. Among the MDM esters 2,3,4-tri-*O*-octanoate **8** (*80.0%) showed highest inhibition followed by 6-*O*-valeroate **4** (*71.6%) and 2,3,6-tri-*O*-valeroate **12** (*71.6%), while the inhibitory activity of standard antibiotic fluconazole was *65.0%. However, only methyl 2,3,4-tri-*O*-octanoyl-6-*O*-valeroate **8** exhibited very good inhibitory activities (*69.7%) against *A. niger*, which was very much better than that of the standard antifungal antibiotic fluconazole (37.1%). More potentiality against fungal pathogens especially *A. fumigatus* by these MDM-based CFA esters are probably due to increased lipophilicity (presence of multiple acyl chains) and glycosidic nature (discussed in SAR section).

2.8. Molecular docking studies

To rationalize the excellent *in vitro* experimental antifungal results of MDM esters 4–12 we conducted their binding affinity with sterol 14 α -demethylase (CYP51). Here, we considered XP docking to filter out the false positive ligand by strict scoring function [41], and used two known reference ligands (VNI; PubChem CID: 49867823, and fluconazole; PubChem CID: 3365) for rigorous validation. Most of the MDM-based CFA esters (**4**, **5**, **7**–**12**) possess higher binding affinity (–7.2 to –11.8 kcal/mol) compared to azole type CYP51 inhibitor fluconazole (–7.147

kcal/mol). These observations clearly supported our PASS and *in vitro* results that the non-azole type MDM esters had better inhibitory potentiality against CYP51 over azole type fluconazole (Table 4).

Interestingly, compound **8** showed the highest negative docking score of –11.836, followed by compound **9** (–10.521) while the docking score for reference ligand VNI was –10.249 and fluconazole was –7.147 only (Table 4). Detail investigation of non-bond interaction of compound **8**, and reference VNI with sterol 14 α -demethylase showed different patterns of bonds. For examples, VNI had one conventional hydrogen bond, one carbon hydrogen bond, two alkyl bonds, and ten pi-alkyl bonds (Fig. 5a). On the other hand, compound **8** showed three conventional hydrogen bonds, one carbon hydrogen bond, ten alkyl bonds, and two pi-alkyl bonds (Figs. 5b and 6). The increased number of conventional hydrogen bonds is a clear indication for a strong binding of compound **8** with sterol 14 α -demethylase. Therefore, the observed profound antimicrobial activity of compound **8** could be originated from the inhibition of sterol 14 α -demethylase which may lead to stop ergosterol synthesis, facilitating leaking of microbial cell membrane.

2.9. MM-GBSA measurement

Molecular mechanics-generalized born surface area (MM-GBSA) measurement indicated that with the addition of multiple ester groups (increasing hydrophobicity), and chain lengths binding affinity with sterol 14 α -demethylase increases (Table S1). To our surprise, more hydrophobic MDM esters **5**–**12** showed better binding affinity with CYP51 than azole type CYP51 inhibitor fluconazole. More importantly, compound **8** had the highest binding affinity (–84.24 kcal/mol) over reference VNI (–83.93 kcal/mol), and fluconazole (–46.58 kcal/mol) (Table S1). These observations clearly revealed that novel compound **8**

Table 3

Zone of inhibition (%) against fungal pathogens by MDM esters.

Percentage of zone of inhibition			
Drug	wt. μ g/mL PDA	<i>A. fumigatus</i>	<i>A. niger</i>
3	100	31.6 \pm 0.34	NI
4	100	*71.7 \pm 0.68	39.4 \pm 0.40
5	100	*70.0 \pm 0.12	24.2 \pm 0.40
6	100	*66.7 \pm 0.49	18.2 \pm 0.33
7	100	*65.0 \pm 0.54	54.5 \pm 0.37
8	100	*80.0 \pm 0.81	*69.7 \pm 0.74
9	100	*70.0 \pm 0.44	51.5 \pm 0.28
10	80	*66.7 \pm 0.58	21.2 \pm 0.37
11	100	*68.3 \pm 0.34	48.5 \pm 0.50
12	100	*71.7 \pm 0.58	18.2 \pm 0.39
FCZ ^[a]	12.5	*65.0 \pm 0.25	37.1 \pm 0.17

Data are presented as Mean \pm SD. FCZ = fluconazole; NI = no inhibition; dw = dry weight; * = good inhibition; [a] standard antibiotic.

Table 4

Extra precision (XP) Glide molecular docking results of MDM esters against sterol 14 α -demethylase.

Drugs	Docking score (kcal/mol)	Glide energy (kcal/mol)	Glide ligand efficiency	Glide emodel (kcal/mol)
8	–11.836	–64.997	–0.257	–98.899
9	–10.521	–67.736	–0.202	–47.747
VNI	–10.249	–57.187	–0.278	–83.708
7	–8.787	–60.802	–0.22	–79.398
11	–8.167	–57.358	–0.221	–79.743
12	–7.63	–49.494	–0.246	–68.819
5	–7.506	–42.097	–0.3	–51.338
10	–7.341	–51.338	–0.237	–71.069
4	–7.218	–36.896	–0.38	–47.944
FCZ	–7.147	–36.927	–0.325	–49.09
6	–6.276	–46.297	–0.224	–53.8
3	–5.704	–21.508	–0.439	–23.063

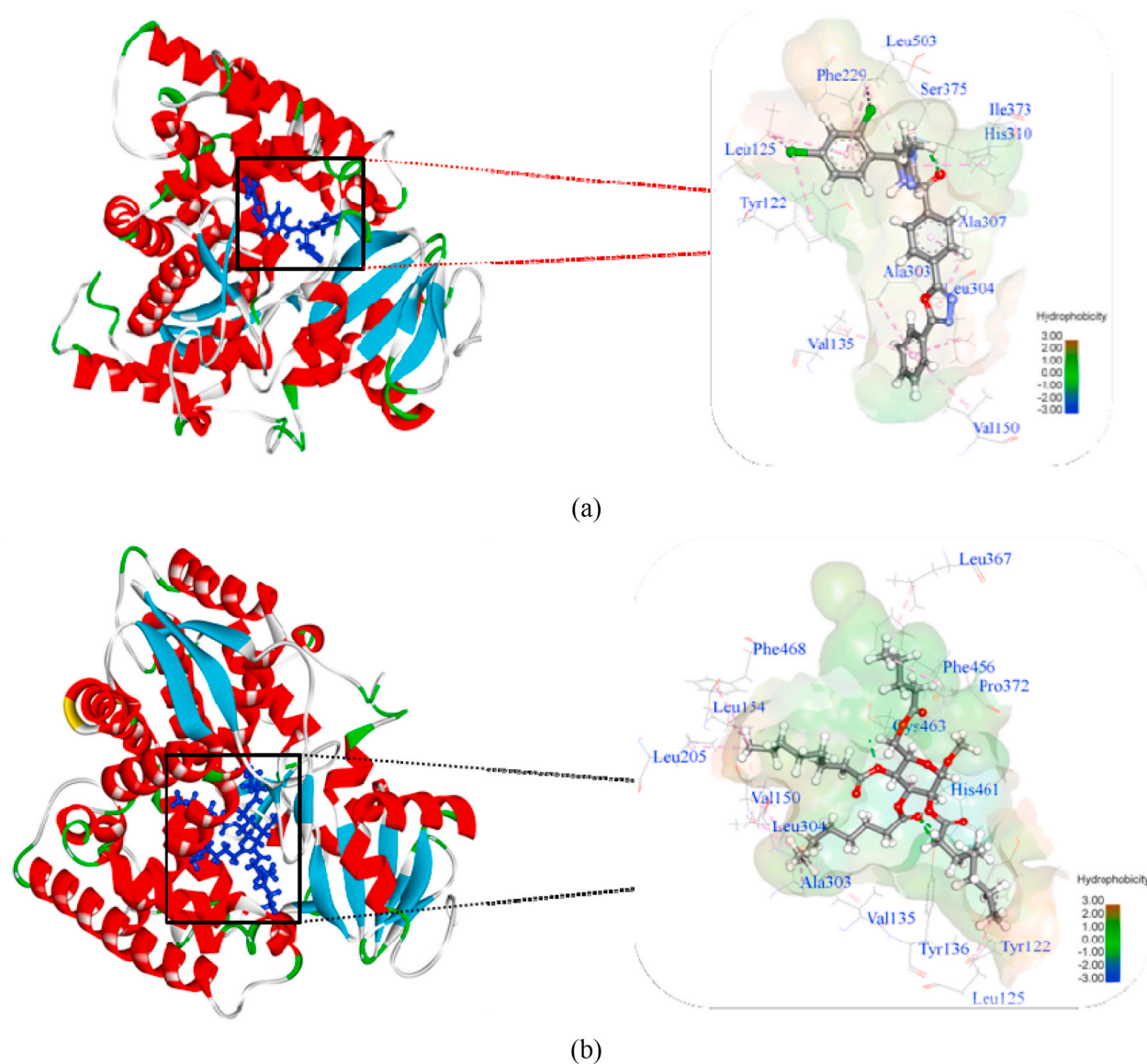


Fig. 5. Binding modes of compounds with sterol 14 α -demethylase. Molecular interactions are displayed in hydrophobic surface view. The hydrophobic intensities of the binding site ranged from -3.00 (least hydrophobic area – shaded blue) to 3.00 (highly hydrophobic area – shaded brown). (a) VNI and sterol 14 α -demethylase complex; (b) compound **8** and sterol 14 α -demethylase complex.

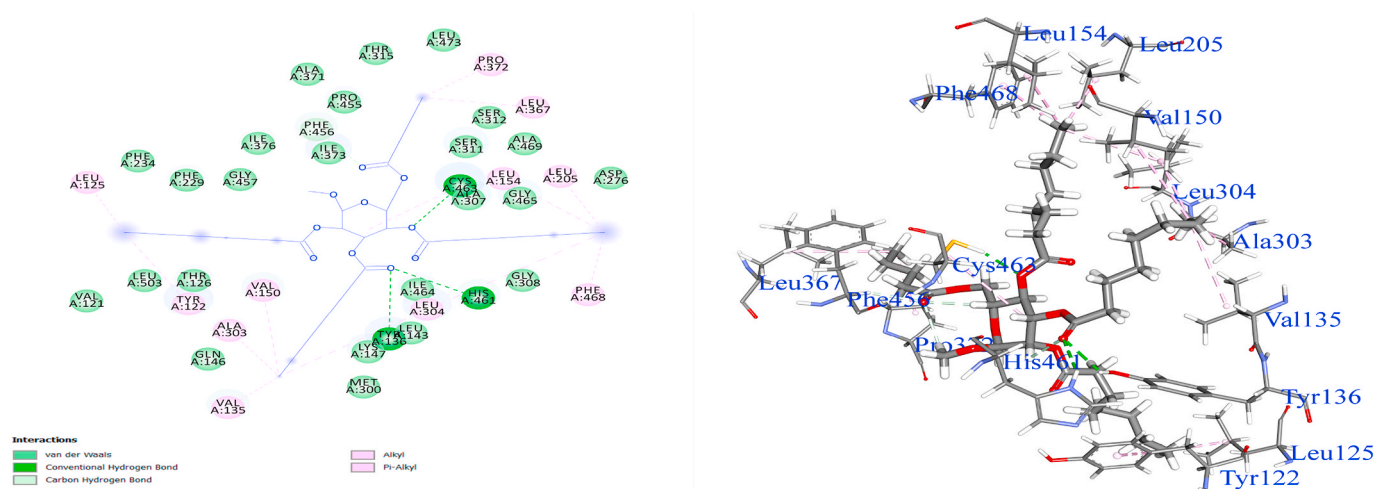


Fig. 6. The best non-bonding interactions of MDM esters **8** in the active site of CYP51 in 2D and 3D style.

may act as competitive inhibitors of sterol 14 α -demethylase (CYP51).

2.10. ADME/T studies

Pharmacokinetic study of the synthetic compounds was conducted using pkCSM [42], (Table S2). First, all MDM esters were water soluble, except compound 7 and 11, and all had a good Caco-2 cell line permeability, except the compound 4 and 5 which were very poorly permeable. All CFA esters showed good intestinal absorption rate and skin permeability, the properties of potential candidates as oral and topical drugs. In addition, most of the MDM esters did not show any noticeable interactions with p-glycoprotein, a biological barrier extruding xenobiotics/drugs reducing the bioavailability of the orally taking drugs [43]. Therefore, all CFA showed overall satisfactory absorption rate.

The volume of distribution (VD) is the theoretical volume that the total dose of a drug would need to be uniformly distributed to give the same concentration as in blood plasma. The higher the VD is the more of a drug is distributed in tissue rather than plasma. Here, VD of all compounds is low. The fraction unbound in plasma is an important determinant of drug efficacy, because in general, only the unbound drug is capable of interacting with pharmacological target proteins such as receptors, channels, and enzymes and is able to diffuse between plasma and tissues. Here, all compounds showing high unbound fraction while SEs 7, 8, and 9 are medium. In addition, CNS permeability and blood brain barrier (BBB) permeability showing similar data, where all compounds are unable to pass CNS and very poorly permeable to BBB, which is important to reduce unusual side effects. Therefore, these CFA esters showed good distribution rate providing high fraction unbound in plasma.

Cytochrome P450 is an important detoxification enzyme in the body; it oxidizes xenobiotics to facilitate their excretion. Many drugs are deactivated by the cytochrome P450, and some can be activated by it. Here, the synthetic compounds did not inhibit the isoforms CYP1A2, CYP2C19, CYP2C9, CYP2D6 and CYP3A4 of cytochrome P450. Interestingly, our synthetic compounds are not likely to be CYP2D6 substrate, but SEs 5–12 metabolite by CYP3A4. These data suggested that these novel CFA esters were not metabolized by maximum isoforms of cytochrome P450. Hence, metabolism of CFA esters showed satisfactory results by avoiding cytochrome P450 metabolism.

Organic cation transporter 2 (OCT2) is a renal uptake transporter that plays an important role in disposition and renal clearance of drugs. Here, all compounds are not likely to be OCT2 substrate, except compounds 7 and 8. Total clearance of drugs is also calculated, which will be helpful for dosing rate of drug. The entire novel SEs did not show any toxicity in AMES toxicity, hepatotoxicity and skin sensitization analyses. They also did not inhibit human ether a go-go gene (hERG) indicating safer drug nature. Inhibition of hERG by any drug causes for the development of acquire long QT syndrome, which lead to fatal

ventricular arrhythmia.

2.10.1. Drug-likeness studies

Pharmaceutically relevant all physicochemical properties of CFA esters like number of heavy atoms, number of aromatic heavy atoms, fraction Csp3, rotatable bonds, number of hydrogen bonds acceptors and donors, molar refractivity (MR), and topological polar surface area (TPSA) were consider for drug-likeness evaluation (Table 5). Different studies reported that number of heavy atoms should be 20 to 70, fraction Csp3 should be > 0.25, rotatable bonds should be \leq 10, number of H-bonds acceptors should be \leq 10, number of H-bonds donors \leq 5, MR should be between 40 and 130 and TPSA should be \leq 140. Further, we considered different computational filter of Lipinski, Ghose, Veber, Egan and Muegge which developed based on different cut off values of physicochemical properties of molecules. Here, compound 9 showed 2 Lipinski violations while 7, 8 and 11 showed 1 violation and rest of the compounds showed 0 violations. All the SEs satisfied Lipinski rule of five except compound 9. Hence, we consider other filter where maximum compounds were satisfied the drug-likeness evaluation and bioavailability score of all compounds satisfied drug-likeness test except C10 chain containing compound 9.

2.11. Structure activity relationship (SAR)

We attempted to derive structure activity relationship (SAR) of the MDM esters on the basis of our PASS, *in vitro* activity tests, docking, and MM-GBSA binding affinity results to shed light into the mechanisms of antimicrobial activity. Firstly, with the addition of mono to multiple ester group(s) and elongation of chain lengths (C2–C10) hydrophobicity of the resulting MDM esters gradually increased. This increased hydrophobicity perhaps could because of the improved hydrophobic membrane permeation [19,22,44] and as a consequence microorganism lose their membrane integrity followed by lysis. Secondly, in general, with the increase of chain length antifungal activity, and binding affinity gradually enhanced up to C8 and then decreases with elongation of chain length (C10) (Tables 2–4).

Overall, it was evident that addition of valeroyl (C5) and octanoyl (C8) groups, especially valeroyl at C-6 position and octanoyl at C-2, C-3 and C-4 positions as in compound 8, increased both docking MM-GBSA binding affinity profoundly with sterol 14 α -demethylase (CYP51; Tables 4 and S1; Figs. 5 and 6). The high affinity with CYP51 compared to VNI, and fluconazole inhibit ergosterol biosynthesis, facilitating leaking of microbial cell membrane. Thus, our experimental results depicted most of these MDM esters as potent antifungal agents via CYP51 inhibition. To this end, we believe that the approaches for new and/or derived non-azole type antimicrobial agents that we report here may pave a way dealing with increased antibiotic resistivity, and may of great interest from global public health viewpoint.

Table 5
Drug-likeness evaluation of CFA esters using SwissADME.

Categories	Parameters	3	4	5	6	7	8	9	10	11	12	
Physico-chemical properties	Heavy atoms	13	19	25	28	40	46	52	31	37	31	
	Aromatic heavy atoms	0	0	0	0	0	0	0	0	0	0	
	Fraction Csp3	1	0.92	0.88	0.78	0.87	0.89	0.9	0.81	0.85	0.86	
	Rotatable bonds	2	7	12	13	25	31	37	16	22	17	
	H-bond acceptors	6	7	8	10	10	10	10	10	10	9	
	H-bond donors	4	3	2	0	0	0	0	0	0	1	
	Molar refractivity	40.47	64.62	88.78	93.84	151.52	180.36	209.2	108.26	137.1	112.94	
	TPSA	99.38	105.45	111.52	123.66	123.66	123.66	123.66	123.66	123.66	117.59	
Drug-likeness filters	Lipinski violations	0	0	0	0	1	1	2	0	1	0	
	Ghose violations	1	1	0	0	3	4	4	0	3	0	
	Veber violations	0	0	1	1	1	1	1	1	1	1	
	Egan violations	0	0	0	0	0	1	1	0	0	0	
	Muegge violations	2	0	0	0	2	3	3	1	2	1	
	Bioavailability Score	0.55	0.55	0.55	0.55	0.55	0.55	0.55	0.17	0.55	0.55	0.55

3. Conclusion

We presented a general and convenient method to synthesize a series of regioselective mannopyranoside based novel CFA esters reasonably in good yields. The applicability of these CFA esters as antimicrobials was tested. Both PASS predication and *in vitro* evaluation established them as better antifungal agent(s) than standard antibiotic. Pharmacokinetic studies like ADME/T, drug-likeness, and medicinal chemistry friendliness analyses revealed that these CFA esters possess good results, and hence, all compounds (except **9**) are oral and topical active candidates. Molecular docking study revealed the detailed binding mode of CFA esters with sterol 14 α -demethylase, where compound **8** showed best binding mode contributing 3 conventional hydrogen bonds. Molecular mechanics-generalized born surface area (MM-GBSA), all computational and SAR study concluded that amongst the saturated acyl chains, valeric chain (C5) in combination with caprylic (C8) chains, as in novel compound **8**, was found the most promising against fungal pathogens, and may act as competitive inhibitors of sterol 14 α -demethylase comparable to fungal antibiotic. It is anticipated that compound **8**, and other structures that emerge in coming years, will provide rationales to address profound CYP51 inhibitory activities with diversity of non-azole type mannopyranoside esters.

4. Experimental section

4.1. Instrumentation and materials

Thin layer chromatography (TLC) was performed on Kieselgel GF₂₅₄ plates and the plates were heated at 150–200 °C by spraying with 1% methanolic H₂SO₄ until coloration took place. Column chromatography (CC) was performed with silica gel G₆₀. Evaporations were conducted below 40 °C in a Buchi rotary evaporator (R-100, Switzerland) under reduced pressure. The solvent system employed for the TLC and CC was chloroform/methanol and/or *n*-hexane/ethyl acetate in different proportions. FT-IR spectra were recorded on a FT-IR spectrophotometer (Shimadzu, IR Prestige-21) in KBr technique. ¹H (400 MHz) and ¹³C (100 MHz) NMR spectra were recorded in CDCl₃ solution using tunable multinuclear probe (Bruker DPX-400 spectrometer, Switzerland). Chemical shifts were reported in δ unit (ppm) maintaining TMS as an internal standard, and *J* values are shown in Hz. Elemental analyses were conducted with a C,H-analyzer. Solvents and commercially available chemicals (Merck) were purified by standard methods or used as purchased.

4.2. Synthesis

4.2.1. Methyl 6-O-valeroyl- α -D-mannopyranoside (**4**)

To a cooled (0 °C) mixture of methyl α -D-mannopyranoside (MDM, **3**) (3.0 g, 15.450 mmol) and pyridine (5 mL) was added valeroyl chloride (pentanoyl chloride) (2.05 g, 17.001 mmol) slowly. The reaction mixture was stirred at 0 °C for 4 h and then overnight at room temperature when TLC indicated the complete conversion of the starting compound into a faster moving product (*R_f* = 0.31, chloroform/methanol = 5:1). Ice was added to the flask to decompose excess reagent. Usual work-up followed by elution with chloroform/methanol (10:1, v/v) provided compound **4** (3.40 g, 79%) as semi-solid. *R_f* = 0.31 (chloroform/methanol = 5:1); FT-IR (KBr) $\nu_{\max}/\text{cm}^{-1}$: 3250–3550 (br OH), 1733 (C=O), 1059 cm^{-1} (pyranose ring). ¹H NMR (400 MHz, CDCl₃): δ_{H} 4.69 (s, 1H, H-1), 4.40 (dd, *J* = 12.2 and 5.0 Hz, 1H, H-6a), 4.22–4.32 (br m, 4H, H-6b and 3 \times OH), 3.92 (dd, *J* = 3.6 and 1.2 Hz, 1H, H-2), 3.78 (dd, *J* = 9.6 and 3.6 Hz, 1H, H-3), 3.69–3.73 (m, 1H, H-5), 3.64 (t, *J* = 9.6 Hz, 1H, H-4), 3.37 (s, 3H, OCH₃), 2.37 [t, *J* = 7.4 Hz, 2H, CH₃(CH₂)₂CH₂CO], 1.55–1.64 (m, 2H, CH₃CH₂CH₂CH₂CO), 1.30–1.40 [m, 2H, CH₃CH₂(CH₂)₂CO], 0.91 [t, *J* = 7.4 Hz, 3H, CH₃(CH₂)₃CO]. ¹³C NMR (100 MHz, CDCl₃): δ_{C} 174.1 [CH₃(CH₂)₃CO], 100.9 (C-1), 71.5, 70.5, 70.4, (C-2/C-3/C-5), 67.7 (C-4), 63.8 (C-6), 54.8 (OCH₃), 34.1

[CH₃(CH₂)₂CH₂CO], 26.9 (CH₃CH₂CH₂CH₂CO), 22.2 [CH₃CH₂(CH₂)₂CO], 13.6 [CH₃(CH₂)₃CO]. Anal. Calcd for C₁₂H₂₂O₇ (278.3): C, 51.79; H, 7.97. Found: C, 51.85; H, 7.99.

4.2.2. Methyl 3,6-di-O-valeroyl- α -D-mannopyranoside (**5**) and methyl 6-O-valeroyl- α -D-mannopyranoside (**4**): DMAP catalyzed valeroylation

Reaction of MDM (**3**, 3.0 g, 15.450 mmol) in dry pyridine (5 mL) with valeroyl chloride (2.05 g, 17.001 mmol) in the presence of catalytic amount of DMAP (10 mg) was conducted at 0 °C for 6 h and 10 h at room temperature. TLC indicated the complete conversion of the starting compound into two faster moving products (*R_f* = 0.59 and 0.31, chloroform/methanol = 5:1). Ice was added to the flask to decompose excess reagent. Usual work-up followed by initial elution with chloroform/methanol (20:1) provided faster-moving component (*R_f* = 0.59) **5** (1.176 g, 21%) as semi-solid which resisted crystallization. *R_f* = 0.59 (chloroform/methanol = 5:1); FT-IR (KBr) $\nu_{\max}/\text{cm}^{-1}$: 3300–3600 (br OH), 1747, 1718 (C=O), 1062 (pyranose ring). ¹H NMR (400 MHz, CDCl₃): δ_{H} 5.11 (dd, *J* = 9.2 and 3.4 Hz, 1H, H-3), 4.80 (d, *J* = 1.2 Hz, 1H, H-1), 4.54 (dd, *J* = 12.2 and 5.6 Hz, 1H, H-6a), 4.31 (dd, *J* = 12.2 and 2.2 Hz, 1H, H-6b), 4.01 (dd, *J* = 2.0 and 3.4 Hz, 1H, H-2), 3.82 (br s, 2H, 2 \times OH), 3.72–3.75 (m, 1H, H-5), 3.62 (t, *J* = 9.6 Hz, 1H, H-4), 3.41 (s, 3H, OCH₃), 2.31–2.45 [m, 4H, 2 \times CH₃(CH₂)₂CH₂CO], 1.60–1.70 (m, 4H, 2 \times CH₃CH₂CH₂CH₂CO), 1.26–1.42 [m, 4H, 2 \times CH₃CH₂(CH₂)₂CO], 0.95 [t, *J* = 7.2 Hz, 3H, CH₃(CH₂)₃CO], 0.92 [t, *J* = 7.2 Hz, 3H, CH₃(CH₂)₃CO]. ¹³C NMR (100 MHz, CDCl₃): δ_{C} 174.1, 173.5 (2 \times CO), 100.7 (C-1), 70.9, 70.5, 69.4 (C-2/C-3/C-5), 66.0 (C-4), 63.1 (C-6), 55.1 (OCH₃), 34.1, 33.9 [2 \times CH₃(CH₂)₂CH₂CO], 27.0, 26.9 (2 \times CH₃CH₂CH₂CH₂CO), 22.2, 22.1 [2 \times CH₃CH₂(CH₂)₂CO], 13.6(2) [2 \times CH₃(CH₂)₃CO]. Anal. Calcd for C₁₇H₃₀O₈ (362.42): C, 56.34; H, 8.34. Found: C, 56.41; H, 8.41.

Further elution with chloroform/methanol (12:1) provided slower-moving component (*R_f* = 0.31, chloroform/methanol = 5:1) **4** (2.021 g, 47%) as semi-solid. Its FT-IR, ¹H and ¹³C NMR spectra were similar to that of prepared by direct valeroylation in the earlier step.

4.2.3. General procedure for 2,3,4-tri-O- and 2,4-di-O-acylation of compound **4** and **5**

To a solution of the **4** or **5** (0.1 g) in dry pyridine (1 mL) corresponding acyl halide (3.3 or 2.2 eq.) was added slowly at 0 °C followed by addition of catalytic amount of DMAP. The reaction mixture was allowed to attain room temperature and stirring was continued for 11–16 h. For compound **9**, the reaction mixture was stirred additional 1 h at 45 °C. A small amount of ice was added to the reaction mixture to decompose excess acyl halide and extracted with dichloromethane (DCM, 5 \times 3 mL). The DCM layer was washed successively with 5% hydrochloric acid, saturated aqueous sodium hydrogen carbonate solution and brine. The DCM layer was dried and concentrated under reduced pressure. The residue thus obtained on CC (gradient elution form *n*-hexane to *n*-hexane/ethyl acetate = 8:1) gave the corresponding 2,3,4-tri-O- or 2,4-di-O-acyl esters.

4.2.4. Methyl 2,3,4-tri-O-acetyl-6-O-valeroyl- α -D-mannopyranoside (**6**)

Syrup; yield 93%; *R_f* = 0.54 (*n*-hexane/EA = 4:1); FT-IR (KBr) $\nu_{\max}/\text{cm}^{-1}$: 1759, 1755, 1738 (C=O), 1087 (pyranose ring). ¹H NMR (400 MHz, CDCl₃): δ_{H} 5.35 (dd, *J* = 8.2 and 3.2 Hz, 1H, H-3), 5.29 (t, *J* = 8.8 Hz, 1H, H-4), 5.25 (dd, *J* = 3.2 and 1.4 Hz, 1H, H-2), 4.72 (d, *J* = 1.4 Hz, 1H, H-1), 4.28 (dd, *J* = 12.0 and 5.6 Hz, 1H, H-6a), 4.14 (dd, *J* = 12.0 and 2.4 Hz, 1H, H-6b), 3.98 (ddd, *J* = 8.8, 5.6 and 2.4 Hz, 1H, H-5), 3.42 (s, 3H, OCH₃), 2.38 [t, *J* = 7.8 Hz, 2H, CH₃(CH₂)₂CH₂CO], 2.16 (s, 3H, CH₃CO), 2.05 (s, 3H, CH₃CO), 2.00 (s, 3H, CH₃CO), 1.60–1.68 (m, 2H, CH₃CH₂CH₂CH₂CO), 1.32–1.40 [m, 2H, CH₃CH₂(CH₂)₂CO], 0.92 [t, *J* = 7.3 Hz, 3H, CH₃(CH₂)₃CO]. ¹³C NMR (100 MHz, CDCl₃): δ_{C} 173.4 [CH₃(CH₂)₃CO], 170.0, 169.8, 169.6 (CH₃CO), 98.6 (C-1), 69.6, 69.2, 68.5, (C-2/C-3/C-5), 66.2 (C-4), 62.3 (C-6), 55.2 (OCH₃), 33.8 [CH₃(CH₂)₂CH₂CO], 26.8 (CH₃CH₂CH₂CH₂CO), 22.2 [CH₃(CH₂)₂CH₂CO], 20.8, 20.7, 20.6 (CH₃CO), 13.6 [CH₃(CH₂)₃CO].

Anal. Calcd for $C_{18}H_{28}O_{10}$ (404.41): C, 53.46; H, 6.98. Found: C, 53.51; H, 6.94.

4.2.5. Methyl 2,3,4-tri-O-hexanoyl-6-O-valeroyl- α -D-mannopyranoside (7)

Semi-solid; yield 86%; $R_f = 0.55$ (*n*-hexane/EA = 4:1); FT-IR (KBr) $\nu_{\max}/\text{cm}^{-1}$: 1739, 1725, 1713, 1695 (C=O), 1068 (pyranose ring). ^1H NMR (400 MHz, CDCl_3): δ_{H} 5.37 (dd, $J = 10.0$ and 3.2 Hz, 1H, H-3), 5.33 (t, $J = 9.6$ Hz, 1H, H-4), 5.27 (dd, $J = 3.2$ and 1.1 Hz, 1H, H-2), 4.70 (d, $J = 1.1$ Hz, 1H, H-1), 4.24 (dd, $J = 12.4$ and 5.6 Hz, 1H, H-6a), 4.15 (dd, $J = 12.4$ and 2.0 Hz, 1H, H-6b), 3.95–4.00 (m, 1H, H-5), 3.41 (s, 3H, OCH₃), 2.32–2.42, 2.18–2.29 [2 × m, 8H, CH₃(CH₂)₂CH₂CO and 3 × CH₃(CH₂)₃CH₂CO], 1.51–1.68 [m, 8H, CH₃CH₂CH₂CH₂CO and 3 × CH₃(CH₂)₂CH₂CH₂CO], 1.23–1.41 [br m, 14H, CH₃CH₂(CH₂)₂CO and 3 × CH₃(CH₂)₂(CH₂)₂CO], 0.86–0.96 [m, 12H, CH₃(CH₂)₃CO and 3 × CH₃(CH₂)₄CO]. ^{13}C NMR (100 MHz, CDCl_3): δ_{C} 173.3, 172.7, 172.5, 172.4 [CH₃(CH₂)₃CO and 3 × CH₃(CH₂)₄CO], 98.7 (C-1), 69.3, 69.0, 68.6, (C-2/C-3/C-5), 65.9 (C-4), 62.4 (C-6), 55.2 (OCH₃), 34.1, 34.0(2), 33.8 [CH₃(CH₂)₂CH₂CO and 3 × CH₃(CH₂)₃CH₂CO], 31.2, 31.1(2) [3 × CH₃(CH₂)₂CH₂CH₂CO], 26.8 (CH₃CH₂CH₂CH₂CO), 24.6, 24.4, 24.3 [3 × CH₃CH₂CH₂(CH₂)₂CO], 22.2, 22.1(3) [CH₃CH₂(CH₂)₂CO and 3 × CH₃CH₂(CH₂)₃CO], 13.8, 13.7(2), 13.6 [CH₃(CH₂)₃CO and 3 × CH₃(CH₂)₄CO]. Anal. Calcd for $C_{30}H_{52}O_{10}$ (572.73): C, 62.91; H, 9.15. Found: C, 62.98; H, 9.18.

4.2.6. Methyl 2,3,4-tri-O-octanoyl-6-O-valeroyl- α -D-mannopyranoside (8)

Oil; yield 82%; $R_f = 0.62$ (*n*-hexane/EA = 4:1); FT-IR (KBr) $\nu_{\max}/\text{cm}^{-1}$: 1738, 1724, 1716, 1689, (C=O), 1068 (pyranose ring). ^1H NMR (400 MHz, CDCl_3): δ_{H} 5.36 (dd, $J = 10.0$ and 3.2 Hz, 1H, H-3), 5.32 (t, $J = 9.6$ Hz, 1H, H-4), 5.27 (dd, $J = 3.2$ and 1.1 Hz, 1H, H-2), 4.71 (d, $J = 1.1$ Hz, 1H, H-1), 4.25 (dd, $J = 12.0$ and 5.6 Hz, 1H, H-6a), 4.16 (dd, $J = 12.0$ and 2.0 Hz, 1H, H-6b), 3.96–3.99 (m, 1H, H-5), 3.42 (s, 3H, OCH₃), 2.36–2.44, 2.19–2.29 [2 × m, 8H, CH₃(CH₂)₂CH₂CO and 3 × CH₃(CH₂)₅CH₂CO], 1.50–1.68 (m, 8H, CH₃CH₂CH₂CH₂CO and 3 × CH₃(CH₂)₄CH₂CH₂CO], 1.20–1.42 [br m, 26H, CH₃CH₂(CH₂)₂CO and 3 × CH₃(CH₂)₄(CH₂)₂CO], 0.87–0.96 [m, 12H, CH₃(CH₂)₃CO and 3 × CH₃(CH₂)₆CO]. ^{13}C NMR (100 MHz, CDCl_3): δ_{C} 173.4, 172.8, 172.5, 172.4 [CH₃(CH₂)₃CO and 3 × CH₃(CH₂)₆CO], 98.7 (C-1), 69.3, 69.0, 68.6, (C-2/C-3/C-5), 65.9 (C-4), 62.4 (C-6), 55.2 (OCH₃), 34.2, 34.1(2), 33.8 [CH₃(CH₂)₂CH₂CO and 3 × CH₃(CH₂)₅CH₂CO], 31.7, 31.6(2) [3 × CH₃(CH₂)₄CH₂CH₂CO], 29.1, 29.0(2), 28.9, 28.8(2) [3 × CH₃(CH₂)₂(CH₂)₂(CH₂)₂CO], 26.8 (CH₃CH₂CH₂CH₂CO), 24.9, 24.8, 24.7 [3 × CH₃CH₂CH₂(CH₂)₄CO], 22.6, 22.5(2), 22.1 [CH₃CH₂(CH₂)₂CO and 3 × CH₃CH₂(CH₂)₅CO], 14.0(3), 13.6 [CH₃(CH₂)₃CO and 3 × CH₃(CH₂)₆CO]. Anal. Calcd for $C_{36}H_{64}O_{10}$ (656.89): C, 65.82; H, 9.82. Found: C, 65.88; H, 9.80.

4.2.7. Methyl 2,3,4-tri-O-decanoyl-6-O-valeroyl- α -D-mannopyranoside (9)

Oil; yield 81%; $R_f = 0.67$ (*n*-hexane/EA = 4:1); FT-IR (KBr) $\nu_{\max}/\text{cm}^{-1}$: 1748, 1713, 1711, 1710 (C=O), 1065 (pyranose ring). ^1H NMR (400 MHz, CDCl_3): δ_{H} 5.36 (dd, $J = 10.0$ and 3.2 Hz, 1H, H-3), 5.31 (t, $J = 9.6$ Hz, 1H, H-4), 5.27 (dd, $J = 3.4$ and 1.2 Hz, 1H, H-2), 4.71 (d, $J = 1.2$ Hz, 1H, H-1), 4.25 (dd, $J = 12.0$ and 5.6 Hz, 1H, H-6a), 4.15 (dd, $J = 12.0$ and 2.0 Hz, 1H, H-6b), 3.96–4.00 (m, 1H, H-5), 3.41 (s, 3H, OCH₃), 2.27–2.43 [m, 8H, CH₃(CH₂)₂CH₂CO and 3 × CH₃(CH₂)₇CH₂CO], 1.56–1.68 [m, 8H, CH₃CH₂CH₂CH₂CO and 3 × CH₃(CH₂)₆CH₂CH₂CO], 1.21–1.42 [br m, 38H, CH₃CH₂(CH₂)₂CO and 3 × CH₃(CH₂)₆(CH₂)₂CO], 0.96 (t, $J = 7.6$ Hz, 3H, CH₃), 0.89 (t, $J = 7.2$ Hz, 9H, 3 × CH₃). ^{13}C NMR (100 MHz, CDCl_3): δ_{C} 173.4, 172.8, 172.5, 172.4 [CH₃(CH₂)₃CO and 3 × CH₃(CH₂)₆CO], 98.7 (C-1), 69.3, 69.0, 68.6, (C-2/C-3/C-5), 65.9 (C-4), 62.4 (C-6), 55.2 (OCH₃), 34.0(4) [CH₃(CH₂)₂CH₂CO and 3 × CH₃(CH₂)₇CH₂CO], 31.9, 31.8(2) [3 × CH₃(CH₂)₆CH₂CH₂CO], 29.4(3), 29.2 (6), 29.0(3) [3 × CH₃(CH₂)₂(CH₂)₄(CH₂)₂CO], 26.8 (CH₃CH₂CH₂CH₂CO), 24.6(3) [3 × CH₃CH₂CH₂(CH₂)₆CO], 22.6(4) [CH₃CH₂(CH₂)₂CO and 3 × CH₃CH₂(CH₂)₇CO], 14.0(4) [CH₃(CH₂)₃CO and 3 × CH₃(CH₂)₈CO]. Anal. Calcd for $C_{42}H_{76}O_{10}$ (741.05): C, 68.07; H, 10.34. Found: C, 68.11; H, 10.38.

4.2.8. Methyl 2,4-di-O-acetyl-3,6-di-O-valeroyl- α -D-mannopyranoside (10)

Thick syrup; yield 89%; $R_f = 0.52$ (*n*-hexane/EA = 4:1); FT-IR (KBr) $\nu_{\max}/\text{cm}^{-1}$: 1763, 1756, 1747, 1733 (C=O), 1086 (pyranose ring). ^1H NMR (400 MHz, CDCl_3): δ_{H} 5.35 (dd, $J = 10.0$ and 3.2 Hz, 1H, H-3), 5.31 (t, $J = 10.0$ Hz, 1H, H-4), 5.24 (dd, $J = 3.2$ and 1.2 Hz, 1H, H-2), 4.71 (d, $J = 1.2$ Hz, 1H, H-1), 4.27 (dd, $J = 12.4$ and 5.6 Hz, 1H, H-6a), 4.16 (dd, $J = 12.4$ and 2.2 Hz, 1H, H-6b), 3.95–3.99 (m, 1H, H-5), 3.41 (s, 3H, OCH₃), 2.22–2.42 [m, 4H, 2 × CH₃(CH₂)₂CH₂CO], 2.15 (s, 3H, CH₃CO), 2.03 (s, 3H, CH₃CO), 1.62–1.68 (m, 2H, CH₃CH₂CH₂CH₂CO), 1.50–1.58 (m, 2H, CH₃CH₂CH₂CH₂CO), 1.26–1.42 [m, 4H, 2 × CH₃CH₂(CH₂)₂CO], 0.95 [t, $J = 7.6$ Hz, 3H, CH₃(CH₂)₃CO], 0.90 [t, $J = 7.2$ Hz, 3H, CH₃(CH₂)₃CO]. ^{13}C NMR (100 MHz, CDCl_3): δ_{C} 173.4, 172.6 [2 × CH₃(CH₂)₃CO], 169.9, 169.6 (2 × CH₃CO), 98.6 (C-1), 69.6, 68.8, 68.5 (C-2/C-3/C-5), 66.2 (C-4), 62.3 (C-6), 55.2 (OCH₃), 33.8, 33.7 [2 × CH₃(CH₂)₂CH₂CO], 26.8, 26.7 (2 × CH₃CH₂CH₂CH₂CO), 22.2, 22.1 [2 × CH₃CH₂(CH₂)₂CO], 20.7, 20.6 (2 × CH₃CO), 13.6, 13.5 [2 × CH₃(CH₂)₃CO]. Anal. Calcd for $C_{21}H_{34}O_{10}$ (446.49): C, 56.49; H, 7.68. Found: C, 56.43; H, 7.72.

4.2.9. Methyl 2,3,4,6-tetra-O-valeroyl- α -D-mannopyranoside (11) and methyl 2,3,6-tri-O-valeroyl- α -D-mannopyranoside (12)

Methyl α -D-mannopyranoside (3) (0.2 g, 1.03 mmol) in pyridine was treated with valeroyl chloride (0.619 g, 4.532 mmol) in presence of catalytic amount of DMAP. The reaction mixture was allowed to attain the room temperature and stirring was continued at room temperature for 12 h and 1 h at 45 °C, when TLC examination indicated the completion of the reaction with the formation of two products ($R_f = 0.58$ and 0.49). Usual work-up and CC purification with *n*-hexane/EA (14:1) initially gave tetra-O-valerate **11** (0.306 g, 56%) as a homogeneous syrup. $R_f = 0.58$ (*n*-hexane/EA = 4:1); FT-IR (KBr) $\nu_{\max}/\text{cm}^{-1}$: 1760, 1741, 1735, 1733 (C=O), 1084 (pyranose ring). ^1H NMR (400 MHz, CDCl_3): δ_{H} 5.32 (dd, $J = 10.0$ and 3.2 Hz, 1H, H-3), 5.28 (t, $J = 10.0$ Hz, 1H, H-4), 5.22 (dd, $J = 3.2$ and 1.2 Hz, 1H, H-2), 4.67 (d, $J = 1.2$ Hz, 1H, H-1), 4.20 (dd, $J = 12.0$ and 5.2 Hz, 1H, H-6a), 4.11 (dd, $J = 12.2$ and 2.4 Hz, 1H, H-6b), 3.92–3.96 (m, 1H, H-5), 3.38 (s, 3H, OCH₃), 2.31–2.38 [m, 4H, 2 × CH₃(CH₂)₂CH₂CO], 2.20–2.27 [m, 2H, CH₃(CH₂)₂CH₂CO], 2.15–2.19 [m, 2H, CH₃(CH₂)₂CH₂CO], 1.57–1.66 [m, 4H, 2 × CH₃CH₂CH₂CH₂CO], 1.52–1.56 [m, 4H, 2 × CH₃CH₂CH₂CH₂CO], 1.21–1.40 [m, 8H, 4 × CH₃CH₂(CH₂)₂CO], 0.91 [t, $J = 7.2$ Hz, 3H, CH₃(CH₂)₃CO], 0.84 [t, $J = 7.2$ Hz, 3H, CH₃(CH₂)₃CO]. ^{13}C NMR (100 MHz, CDCl_3): δ_{C} 173.3, 172.7, 172.5, 172.3 [4 × CH₃(CH₂)₃CO], 98.6 (C-1), 69.3, 69.0, 68.6, (C-2/C-3/C-5), 65.8 (C-4), 62.3 (C-6), 55.2 (OCH₃), 33.8, 33.7(3) [4 × CH₃(CH₂)₂CH₂CO], 26.9, 26.8, 26.7, 26.6 (4 × CH₃CH₂CH₂CH₂CO), 22.2, 22.1, 22.0(2) [4 × CH₃CH₂(CH₂)₂CO], 13.6, 13.5(3) [4 × CH₃(CH₂)₃CO]. Anal. Calcd for $C_{27}H_{46}O_{10}$ (530.65): C, 61.11; H, 8.74. Found: C, 61.17; H, 8.77.

Further elution with *n*-hexane/EA (10:1, v/v) furnished tri-O-valerate **12** (0.120 g, 26%) as a homogeneous syrup. $R_f = 0.49$ (*n*-hexane/EA = 4:1); FT-IR (KBr) $\nu_{\max}/\text{cm}^{-1}$: 3308–3560 (OH), 1738, 1733, 1730 (C=O), 1081 (pyranose ring). ^1H NMR (400 MHz, CDCl_3): δ_{H} 5.20 (dd, $J = 3.6$ and 1.0 Hz, 1H, H-2), 5.16 (dd, $J = 10.0$ and 3.6 Hz, 1H, H-3), 4.65 (d, $J = 1.0$ Hz, 1H, H-1), 4.46 (dd, $J = 12.0$ and 4.2 Hz, 1H, H-6a), 4.33 (dd, $J = 12.2$ and 2.4 Hz, 1H, H-6b), 3.80–3.84 (m, 1H, H-5), 3.78 (t, $J = 10.0$ Hz, 1H, H-4), 3.38 (s, 3H, OCH₃), 2.26–2.39 [m, 6H, 3 × CH₃(CH₂)₂CH₂CO], 1.53–1.67 [m, 6H, 3 × CH₃CH₂CH₂CH₂CO], 1.23–1.40 [m, 6H, 3 × CH₃CH₂(CH₂)₂CO], 0.92 [t, $J = 7.2$ Hz, 6H, CH₃(CH₂)₃CO], 0.88 [t, $J = 7.6$ Hz, 3H, CH₃(CH₂)₃CO]. ^{13}C NMR (100 MHz, CDCl_3): δ_{C} 174.3, 173.6, 172.7 [3 × CH₃(CH₂)₃CO], 98.7 (C-1), 71.4, 70.9, 69.5 (C-2/C-3/C-5), 65.9 (C-4), 63.1 (C-6), 55.1 (OCH₃), 33.9(2), 33.8 [3 × CH₃(CH₂)₂CH₂CO], 27.0, 26.9, 26.7 (3 × CH₃CH₂CH₂CH₂CO), 22.2, 22.1(2) [3 × CH₃CH₂(CH₂)₂CO], 13.6(3) [3 × CH₃(CH₂)₃CO]. Anal. Calcd for $C_{22}H_{38}O_9$ (446.53): C, 59.18; H, 8.58. Found: C, 59.20; H, 8.55.

4.3. *In vitro* antimicrobial activities evaluation

The antibacterial activities of synthesized MDM esters were tested against three human pathogenic bacteria. Among them one Gram-positive was *Staphylococcus aureus* ATCC 25923, and two Gram-negative were *Escherichia coli* ATCC 25922 and *Pseudomonas aeruginosa* (CRL, ICDDR, B). For antibacterial activities test, the disc diffusion method [9,22] was followed. Dimethylformamide (DMF) was used as a solvent for the test chemicals, and a 2% solution of each compound was used. The plates were incubated at 37 °C for 48 h. The control was DMF without chemicals. Mueller-Hinton (agar and broth) medium was used to culture the bacteria. Each experiment was carried out three times. Tetracycline (antibiotic used for bacterial infections, brand name Tetrax-500, from Square Pharmaceuticals Ltd., Bangladesh) was used as a positive control and compared with tested chemicals under identical conditions.

In vitro antifungal activities were investigated against two human pathogenic fungi viz. *Aspergillus fumigatus* ATCC 46645 and *Aspergillus niger* ATCC 16404. The antifungal efficacy was investigated based on food poisoning technique [9,22]. The test tube cultures of the bacterial and fungal pathogens were collected from the Biochemistry Laboratory, Department of Biochemistry and Molecular Biology, University of Chittagong, Bangladesh. Sabouraud (agar and broth, PDA) medium was used for culture of fungi. Linear mycelial growth of fungus was measured after 2–4 days of incubation. The antifungal results were compared with that of standard antibiotic, fluconazole (brand name Omastin, 50 mg, Beximco Pharmaceuticals Ltd., Bangladesh).

4.4. Computational methods

4.4.1. Molecular docking

Cytochrome P450 sterol 14 α -demethylase is the enzyme that catalyzes 14 α demethylation of lanosterol, which is important in ergosterol biosynthesis [45]. Inhibition of this enzyme stopped ergosterol synthesis, which further facilitates cell membrane to rupture in microorganisms. Currently, voriconazole is the drug of choice, though the treatment efficiency is low. For this reason, we have docked these synthetic compounds with Cytochrome P450 sterol 14 α -demethylase to evaluate their binding affinity and compare docking score and non-bond interaction with bounded VNI ligand, and known drug fluconazole.

4.4.1.1. Ligand preparation. In order to build a data set, we have collected SDF format of these synthetic compounds after drawing in ChemDraw 18.0 and we also downloaded SDF format of VNI (PubChem CID: 49867823) and Fluconazole (PubChem CID: 3365) from PubChem database. Further, all the SDF prepared by using LigPrep module 3.1 of Maestro 11.6 software (Maestro, version 11.6, Schrödinger, LLC). Here, all ligands were minimized by applying OPLS3e force field. During the minimization, the module Epik 2.2 was utilized to fix the ionization state of the ligand at pH 7.0 \pm 2.0. From this analysis, up to 32 possible stereoisomers of each compound were generated and we selected the best conformer with lowest energy.

4.4.1.2. Protein preparation. As the protein target of the molecular docking was Cytochrome P450 sterol 14 α -demethylase, its crystal structure was retrieved from the RCSB protein data bank (PDB id: 4UYL; organism: *Aspergillus fumigatus*). Further, the protein crystal structure 4UYL prepared by using protein preparation wizard of Maestro 11.6 software (Maestro, version 11.6, Schrödinger, LLC), in which the crystal structure is initially assigned proper hydrogen, charges and bond orders. At neutral pH, all hydrogen bonds in the structure were optimized, deleting unnecessary water. Then the minimization process was run with the OPLS3e force field, considering structural changes of not more than 0.30 Å of RMSD. The active site of the protein was fixed for docking simulation by generating a grid box at the reference ligand (VNI)

binding site. Grid generation parameters were kept at default, with a box size of 18 Å \times 18 Å \times 18 Å, and the OPLS3e force field utilized for post minimization. The charge cut-off and van der Waals scaling factor were set to 0.25 and 1.00, respectively.

4.4.1.3. Molecular docking procedure. We carried out extra precision (XP) flexible docking using the Glide module of Maestro 11.6 software (Maestro, version 11.6, Schrödinger, LLC), which is more sophisticated than SP/HTVS in scoring function. Here, all ligands were treated flexibly, considering the partial charge and van der Waals factor of 0.15 and 0.80, respectively. Minimization was performed to the docked complex after docking using the OPLS3e force field. The best-docked pose with highest negative Glide score value was recorded for each ligand.

4.4.2. MM-GBSA binding energy measurement

Binding affinity calculations were carried out using the Prime MM-GBSA module of the Maestro 11.6 software (Maestro, version 11.6, Schrödinger, LLC), where greater negative affinity denotes higher stability [46]. The docked Pose viewer file from Glide XP docking was used for calculation, using the sampling minimization protocol used generalized born surface accessible (GBSA) as a continuum model, and OPLS3e force field as molecular mechanics (MM), keeping the protein flexible. For correcting empirical functions of π -stacking and H-bond interactions, a dielectric solvent model such as VSGB 2.0 was used. For comparison binding affinity of CFA esters was compared with standard sterol 14 α -demethylase (CYP51; Table S2) inhibitor VNI (the experimental drug for treatment of Chagas disease caused by the fungus *Trypanosoma*).

4.4.3. ADME/T and drug-likeness evaluation

In order to predict the pharmacokinetic profile of the derivatives, pkCSM online tool [42] was utilized, where the absorption, distribution, metabolism, excretion and toxicity of each ligand were calculated. Drug-likeness and medicinal chemistry friendliness properties of the derivatives, such as topological polar surface area (TPSA), Ghose violation, bioavailability score and Lipinski's rule of five were predicted by using SwissADME web tool [47]. Before using these tools, at first, we have drawn all the structures by ChemDraw 18.0 software, and collected InChI key, SMILES and SD file format. InChI key were used to find these compounds in different database and we found our derivatives as not reported in any database yet. SMILES (simplified molecular-input line-entry system) strings were used in pkCSM, and SwissADME online tools while SD file format used in molecular docking.

Declaration of competing interest

The authors declare that they have no known competing financial interests or personal relationships that could have appeared to influence the work reported in this paper.

Acknowledgements

We highly acknowledge the financial support from the Ministry of Education, Bangladesh and BANBEIS (grant no. PS 201660, 2016–17).

Abbreviations

MDM	methyl α -D-mannopyranoside
CYP	cytochrome P450
CYP51	sterol 14 α -demethylase
SAR	structure activity relationship
CFA	carbohydrate fatty acid
SEs	sugar esters
MDR	multiple drug resistant
MRSA	methicillin-resistant <i>Staphylococcus aureus</i>

DMAP	4-dimethylaminopyridine
PASS	prediction of activity spectra for substances
MM-GBSA	molecular mechanics-generalized born surface area
ADMET	absorption, distribution, metabolism, and excretion
NMR	nuclear magnetic resonance
COSY	correlation spectroscopy
HSQC	heteronuclear single quantum coherence spectroscopy
HMBC	heteronuclear multiple bond correlation
XP	extra precision
VD	volume of distribution
BBB	blood brain barrier
hERG	human ether a go-go gene
MR	molar refractivity
TPSA	topological polar surface area
TLC	thin layer chromatography
CC	column chromatography
TMS	tetramethyl silane
DMF:	dimethylformamide
ATCC	American type culture collection
ICDDR,B	international centre for diarrhoeal disease research, Bangladesh
PDA	potato dextrose agar
SDF	standard data format

Appendix A. Supplementary data

Supplementary data to this article can be found online at <https://doi.org/10.1016/j.carres.2020.108130>.

References

- J.J. Kabara, M. Swieczkowski, A.J. Conley, J.P. Traunt, Fatty acids and derivatives as antimicrobial agents, *Antimicrob. Agents Chemother.* 2 (1972) 23–28, <https://doi.org/10.1128/AAC.2.1.23>.
- J.J. Kabara, A.J. Conley, D.M. Swieczkowski, I.A. Ismail, M.L.K. Jie, F.D. Gunstone, Antimicrobial action of isomeric fatty acids on group A *Streptococcus*, *J. Med. Chem.* 16 (1973) 1060–1063.
- P. Degn, W. Zimmermann, Optimization of carbohydrate fatty acid ester synthesis in organic media by a lipase from *Candida Antarctica*, *Biotechnol. Bioeng.* 74 (2001) 483–491, <https://doi.org/10.1002/bit.1139>.
- A. Szüts, E. Pallagi, G. Regdon, Z. Aigner, P.S.-Révész, Study of thermal behaviour of sugar esters, *Int. J. Pharm.* 336 (2007) 199–207, <https://doi.org/10.1016/j.ijpharm.2006.11.053>.
- D.L. Marshall, L.B. Bullermann, Antimicrobial Properties of Sucrose Fatty Acid Esters, in: C.C. Akoh, B.G. Swanson (Eds.), *Carbohydrate Polymers as Fat Substitutes*, Marcel Dekker, New York, 1994, pp. 149–167.
- S.W. Chang, J.F. Shaw, Biocatalysis for the production of carbohydrate esters, *N. Biotech.* 26 (2009) 109–116, <https://doi.org/10.1016/j.nbt.2009.07.003>.
- S. Okabe, M. Suganuma, Y. Tada, Y. Ochiai, E. Sueoka, H. Kohya, A. Shibata, M. Takahashi, M. Mizutani, T. Matsuzaki, H. Fujiki, Disaccharide esters screened for inhibition of tumor necrosis factor- α release are new anti-cancer agents, *Jpn. J. Canc. Res.* 90 (1999) 669–676, <https://doi.org/10.1111/j.1349-7006.1999.tb00799.x>.
- G.J. Puterka, W. Farone, T. Palmer, A. Barrington, Structure-function relationships affecting the insecticidal and miticidal activity of sugar esters, *J. Econ. Entomol.* 96 (3) (2003) 636–644, <https://doi.org/10.1093/jee/96.3.636>.
- A.K.M.S. Kabir, M.M. Matin, A.F.M. Sanaullah, M.A. Sattar, M.S. Rahman, Antimicrobial activities of some lyxoside derivatives, *Bangladesh J. Microbiol.* 18 (1) (2001) 89–95.
- M.M. Matin, M.M.H. Bhuiyan, A.K.M.S. Azad, S.C. Bhattacharjee, M.H.O. Rashid, Synthesis and antimicrobial studies of 6-O-lauroyl-1,2-O-isopropylidene- α -D-glucopyranose derivatives, *Chem. Biol. Interface* 4 (4) (2014) 223–231.
- R.K. Singh, P. Gupta, O.P. Sharma, S.S. Ray, Homogeneous synthesis of cellulose fatty esters in ionic liquid (1-butyl-3-methylimidazolium chloride) and study of their comparative antifriction property, *J. Ind. Eng. Chem.* 24 (2015) 14–19.
- A.K.M.S. Kabir, M.M. Matin, M.M.R. Bhuiyan, M.A. Rahim, M.S. Rahman, Biological evaluation of some monosaccharide derivatives, *Int. J. Agric. Biol.* 7 (2) (2005) 218–221.
- D.D. Dhavale, M.M. Matin, Selective sulfonylation of 4-C-hydroxymethyl- β -L-threo-pento-1,4-furanose: synthesis of bicyclic diazasugars, *Tetrahedron* 60 (19) (2004) 4275–4281, <https://doi.org/10.1016/j.tet.2004.03.034>.
- M.M. Matin, Synthesis of D-glucose derived oxetane: 1,2-O-isopropylidene-4-(S)-3-O,4-C-methylene-5-O-methanesulfonyl- α -L-threo-pento-1,4-furanose, *J. Appl. Sci. Res.* 4 (11) (2008) 1478–1482.
- M.M. Matin, One step intramolecular cyclization of diol via mesylation: efficient synthesis of sugar derived [1,4]oxazepanes, *J. Bangladesh Chem. Soc.* 21 (2) (2008) 179–183.
- S.S. Yuan, M.L. Li, J.S. Chen, L. Zhou, W. Zhou, Application of mono- or disaccharides in drug targeting and efficacy, *ChemMedChem* 13 (2018) 764–778, <https://doi.org/10.1002/cmdc.201700762>.
- C.Y. New, A.R. Amalia, O.S.B. Ramzi, R. Son, Antibiotic resistance evolution of methicillin resistant *Staphylococcus aureus* (MRSA) and colloidal silver as the nanoweapon, *Int. Food Res. J.* 23 (2016) 1248–1254.
- M.N. AlFindee, Q. Zhang, Y.P. Subedi, J.P. Shrestha, Y. Kawasaki, M. Grilley, J. Y. Taemoto, C.W.T. Chang, One-step synthesis of carbohydrate esters as antibacterial and antifungal agents, *Bioorg. Med. Chem.* 26 (2018) 765–774, <https://doi.org/10.1016/j.bmc.2017.12.038>.
- M.M. Matin, S.C. Bhattacharjee, P. Chakraborty, M.S. Alam, Synthesis, PASS prediction, *in vitro* antimicrobial evaluation and pharmacokinetic study of novel *n*-octyl glucopyranoside esters, *Carbohydr. Res.* 485 (2019), <https://doi.org/10.1016/j.carres.2019.107812>, 107812.
- J. Lawandi, S. Rocheleau, N. Moitessier, Regioselective acylation, alkylation, silylation and glycosylation of monosaccharides, *Tetrahedron* 72 (2016) 6283–6319, <https://doi.org/10.1016/j.tet.2016.08.019>.
- G.L. Tolnia, U.J. Nilsson, B. Olofsson, Efficient O-functionalization of carbohydrates with electrophilic reagents, *Angew. Chem. Int. Ed.* 55 (2016) 11226–11230, <https://doi.org/10.1002/anie.201605999>.
- M.M. Matin, M.M.H. Bhuiyan, E. Kabir, A.F.M. Sanaullah, M.A. Rahman, M. E. Hossain, M. Uzzaman, Synthesis, characterization, ADMET, PASS prediction, and antimicrobial study of 6-O-lauroyl mannopyranosides, *J. Mol. Struct.* 1195 (2019) 189–197, <https://doi.org/10.1016/j.molstruc.2019.05.102>.
- M.M. Matin, M.M.H. Bhuiyan, A.K.M.S. Azad, M.H.O. Rashid, Synthesis of 6-O-stearoyl-1,2-O-isopropylidene- α -D-glucopyranose derivatives for antimicrobial evaluation, *J. Phys. Sci.* 26 (1) (2015) 1–12.
- M.M. Matin, M.M.H. Bhuiyan, D.C. Debnath, M.A. Manchur, Synthesis and comparative antimicrobial studies of some acylated D-glucopyranose and D-glucopyranose derivatives, *Int. J. Biosci.* 3 (8) (2013) 279–287, <https://doi.org/10.12692/ijb/3.8.279-287>.
- M.M. Matin, M.M.H. Bhuiyan, A.K.M.S. Azad, N. Akther, Design and synthesis of benzyl 4-O-lauroyl- α -L-rhamnopyranoside derivatives as antimicrobial agents, *Curr. Chem. Lett.* 6 (1) (2017) 31–40, <https://doi.org/10.5267/j.ccl.2016.10.001>.
- M.M. Matin, Synthesis and antimicrobial study of some methyl 4-O-palmitoyl- α -L-rhamnopyranoside derivatives, *Orbital: the Electron, J. Chem.* 6 (1) (2014) 20–28, <https://doi.org/10.17807/orbital.v6i1.553>.
- M.M. Matin, A.R. Nath, O. Saad, M.M.H. Bhuiyan, S.B.A. Hamid, A.A. Alhadi, F. A. Kadir, M.E. Ali, W.A. Yehye, Synthesis, PASS-predication and *in vitro* antimicrobial activity of benzyl 4-O-benzoyl- α -L-rhamnopyranoside derivatives, *Int. J. Mol. Sci.* 17 (9) (2016) 1412, <https://doi.org/10.3390/ijms17091412>.
- A.K.M.S. Kabir, M.M. Matin, Regioselective acylation of a derivative of L-rhamnose using the dibutyltin oxide method, *J. Bangladesh Chem. Soc.* 7 (1) (1994) 73–79.
- A.K.M.S. Kabir, M.M. Matin, M.R. Uddin, Comparative studies on selective acylation of uridine using the dibutyltin oxide and direct methods, *Chittagong Univ. J. Sci.* 22 (1) (1998) 97–103.
- A.K.M.S. Kabir, M.M. Matin, Regioselective monoacylation of a derivative of L-rhamnose, *J. Bangladesh Acad. Sci.* 21 (1) (1997) 83–88.
- Á.D.-Ortiz, P. Prieto, A. delaHoz, A critical overview on the effect of microwave irradiation in organic synthesis, *Chem. Rec.* 19 (1) (2019) 85–97, <https://doi.org/10.1002/tcr.201800059>.
- T. Kobayashi, Lipase-catalyzed syntheses of sugar esters in non-aqueous media, *Biotechnol. Lett.* 33 (2011) 1911–1919, <https://doi.org/10.1007/s10529-011-0663-z>.
- D.A. MacManus, E.N. Vulfson, Substituent effects on the regioselectivity of enzymatic acylation of 6-O-alkylglycopyranosides using *Pseudomonas cepacia* lipase, *Carbohydr. Res.* 279 (1995) 281–291, [https://doi.org/10.1016/0008-6215\(95\)00292-8](https://doi.org/10.1016/0008-6215(95)00292-8).
- (a) G.I. Lepesheva, M.R. Waterman, Sterol 14 α -demethylase cytochrome P450 (CYP51), a P450 in all biological kingdoms, *Biochim. Biophys. Acta* 1770 (2007) 467–477, <https://doi.org/10.1016/j.bbagen.2006.07.018>;
(b) M.M. Matin, M.S. Hasan, M. Uzzaman, M.M.H. Bhuiyan, S.M. Kibria, M. E. Hossain, M.H.O. Roshid, Synthesis, spectroscopic characterization, molecular docking, and ADMET studies of mannopyranoside esters as antimicrobial agents, *J. Mol. Struct.* 1222 (2020), <https://doi.org/10.1016/j.molstruc.2020.128821>.
- (a) A. Singh, S.K. Paliwal, M. Sharma, A. Mittal, S. Sharma, J.P. Sharma, *In Silico* and *in vitro* screening to identify structurally diverse non-azole CYP51 inhibitors as potent antifungal agent, *J. Mol. Graph. Model.* 63 (2016) 1–7, <https://doi.org/10.1016/j.jmgl.2015.10.014>;
(b) M.M. Matin, M.H.O. Roshid, S.C. Bhattacharjee, A.K.M.S. Azad, PASS prediction, antiviral, *in vitro* Antimicrobial, and ADMET studies of rhamnopyranoside esters, *Med. Reserve. Arch.* 8 (7) (2020) 2165, <https://doi.org/10.18103/mra.v8i7.2165>.
- T.B. de Souza, A.C.O. Bretas, R.J. Alves, T.F.F. Magalhães, M.A.R. Stoianoff, Synthesis and antifungal activity of palmitic acid-based neoglycolipids related to papulacandin D, *Quim. Nova* 38 (10) (2015) 1282–1288, <https://doi.org/10.5935/0100-4042.20150156>.
- J.J. Reina, A.D. Maio, J.R.-Soriano, R.C. Figueiredob, J. Rojo, Rapid and efficient synthesis of α (1–2) mannobiosides, *Org. Biomol. Chem.* 14 (2016) 2873–2882, <https://doi.org/10.1039/c6ob00083e>.
- A.K.M.S. Kabir, M.M. Matin, M.M. Rahman, Selective benzylation of methyl α -D-mannopyranoside using the dibutyltin oxide and direct methods, *Chittagong Univ. Stud. Part II Sci.* 20 (2) (1996) 99–104.
- S. Marchesan, D. Macmillan, Chemoenzymatic synthesis of GDP-azidodeoxymannoses: non-radioactive probes for mannosyltransferase activity,

- Chem. Commun. (J. Chem. Soc. Sect. D) 36 (2008) 4321–4323, <https://doi.org/10.1039/B807016D>.
- [40] (a) A.R. Fersht, W.P. Jencks, Acetylpyridinium ion intermediate in pyridine-catalyzed hydrolysis and acyl transfer reactions of acetic anhydride. Observation, kinetics, structure-reactivity correlations, and effects of concentrated salt solutions, *J. Am. Chem. Soc.* 92 (1970) 5432–5442, <https://doi.org/10.1021/ja00721a023>; (b) Y. Luan, J. Zhang, M. Zhan, J. Wu, J. Zhang, J. He, Highly efficient propionylation and butyralation of cellulose in an ionic liquid catalyzed by 4-dimethyliminopyridine, *Carbohydr. Polym.* 92 (2013) 307–311, <https://doi.org/10.1016/j.carbpol.2012.08.111>.
- [41] V. Aparna, K. Dineshkumar, N. Mohanalakshmi, D. Velmurugan, W. Hopper, Identification of natural compound inhibitors for multidrug efflux pumps of *Escherichia coli* and *Pseudomonas aeruginosa* using in silico high-throughput virtual screening and in vitro validation, *PLoS One* 9 (2014), e101840, <https://doi.org/10.1371/journal.pone.0101840>.
- [42] D.E. Pires, T.L. Blundell, D.B. Ascher, pkCSM, Predicting small-molecule pharmacokinetic and toxicity properties using graph-based signatures, *J. Med. Chem.* 58 (2015) 4066–4072, <https://doi.org/10.1021/acs.jmedchem.5b00104>.
- [43] J.H. Lin, M. Yamazaki, *Clin Pharmacokinet. Role of P-glycoprotein in pharmacokinetics: clinical implications*, 2003, <https://doi.org/10.2165/00003088-200342010-00003>, 42, 59–98.
- [44] W.A. Hunt, The effects of aliphatic alcohols on the biophysical and biochemical correlates of membrane function, *Adv. Exp. Med. Biol.* 56 (1975) 195–210, https://doi.org/10.1007/978-1-4684-7529-6_9.
- [45] K. Homma, Y. Yoshida, A. Nakano, Evidence for recycling of cytochrome P450 sterol 14-demethylase from the cis-Golgi compartment to the endoplasmic reticulum (ER) upon saturation of the ER-retention mechanism, *J. Biochem.* 127 (2000) 747–754.
- [46] S. Genheden, U. Ryde, The MM/PBSA and MM/GBSA methods to estimate ligand-binding affinities, *Expert Opin. Drug Discov.* 10 (2015) 449–461, <https://doi.org/10.1517/17460441.2015.1032936>.
- [47] A. Daina, O. Michielin, V. Zoete, SwissADME: a free web tool to evaluate pharmacokinetics, drug-likeness and medicinal chemistry friendliness of small molecules, *Sci. Rep.* 7 (2017), <https://doi.org/10.1038/srep42717>, 42717.